Searching for decaying and annihilating dark matter with line intensity mapping

Cyril Creque-Sarbinowski and Marc Kamionkowski

Phys. Rev. D **98**, 063524 — Published 20 September 2018

DOI: 10.1103/PhysRevD.98.063524

Searching for Decaying and Annihilating Dark Matter with Line Intensity Mapping

Cyril Creque-Sarbinowski and Marc Kamionkowski[1, *]

[1] *Department of Physics and Astronomy, Johns Hopkins University, 3400 N. Charles St., Baltimore, MD 21218, USA*

The purpose of line-intensity mapping (IM), an emerging tool for extragalactic astronomy and cosmology, is to measure the integrated emission along the line of sight from spectral lines emitted from galaxies and the intergalactic medium. The observed frequency of the line then provides a distance determination allowing the three-dimensional distribution of the emitters to be mapped. Here we discuss the possibility to use these measurements to seek monoenergetic photons from dark-matter decay or possibly annihilation. The photons from decays or annihilations (should such lines arise) will be correlated with the mass distribution, which can be determined from galaxy surveys, weak-lensing surveys, or the IM mapping experiments themselves. We discuss how to seek this cross-correlation and then estimate the sensitivity of various IM experiments in the dark-matter mass-lifetime parameter space. We find prospects for improvements of nine orders of magnitude in sensitivity to decaying/annihilating dark matter in the frequency bands targeted for IM experiments.

I. INTRODUCTION

Measurements of the cosmic microwave background (CMB) temperature and polarization angular power spectra agree at the percent level with the predictions of ΛCDM, a six-parameter phenomenological model [1, 2]. However, the nature of the cold dark matter required by the model remains a mystery. It could be primordial black holes [3–5], axions [6–10], sterile neutrinos [11], weakly interacting massive particles [12–14], something related to baryons [15], or any of a rich array of other possibilities [16]. There is, however, no prevailing frontrunner among this vast assemblage of ideas, and so any empirical avenue that might provide some hint to the nature of dark matter should be pursued.

In some scenarios a feeble, but nonzero, electromagnetic coupling of the dark-matter particle allows it to decay to a photon line. For example, the axion undergoes two-photon decay, and there are ideas (e.g., axion-mediated dark-photon mixing [17–20]) in which the standard axion phenomenology may be extended. Monoenergetic photons may be emitted in the decay of sterile-neutrino dark matter [11], and there are other ideas (e.g., exciting dark matter [21]) in which two dark-matter states are connected by emission of a photon of some fixed energy. It is also conceivable that monoenergetic photons might be produced in dark-matter annihilation. These possibilities have fueled an extensive search for cosmic-background photons from dark-matter decays or annihilations at an array of frequencies through an array of techniques, among them searches in the extragalactic background light [22–24].

In this paper, we propose to use line-intensity mapping (IM) [25–27], an emerging technique in observational cosmology, to seek radiative dark-matter decays/annihilations in the extragalactic background light. Intensity-mapping experiments measure the brightness of a given galactic emission line as a function of position on the sky and observer frequency (which provides a proxy for the distance) to infer the three-dimensional distribution of the emitters. A considerable intensity-mapping effort with neutral hydrogen's 21-cm line is already underway [35], and efforts are now afoot to develop analogous capabilities with CO and CII molecular lines, hydrogen's Hα line (e.g., with SPHEREx [39], now in a NASA Phase A MidEx study), and others. If dark matter decays or annihilates to a line, the resulting photons will be correlated with the mass distribution, which can be inferred from galaxy surveys, weak-gravitational-lensing maps, or from the intensity-mapping surveys themselves.

Our work follows in spirit Refs. [28, 29], who sought a cross-correlation of an axion decay line with the mass distribution within a given galaxy cluster, but substitutes the cosmic mass distribution for the mass distribution within an individual cluster. We extend on Ref. [30] which sought angular infrared-background-light fluctuations from dark-matter decay, by our inclusion of frequency dependence and cross-correlation with the three-dimensional mass distribution. We take here a theorist's perspective, initially exploring possibilities limited only by astrophysical backgrounds and assuming perfect measurements. Doing so, we find the potential for improvements over current sensitivities of up to nine orders of magnitude, in frequency bands targeted by forthcoming IM efforts. We then show that the improvements in sensitivity are still dramatic even after taking into account the effects of realistic instrumental noise.

This paper is organized as follows: In Section II we discuss the basic idea and make some simple estimates. Section III then adds several additional ingredients required to make connection with realistic experiments. We moreover provide here quantitative estimates for several representative experiments. The results are discussed in Section IV. We discuss briefly particle-physics models the search may be relevant for and show, for example, that SPHEREx has potential to probe hitherto unexplored regions of the axion coupling for axion masses $\sim$ eV.

* creque@jhu.edu; kamion@jhu.edu

II. CALCULATION

Consider a Big Bang relic of mass m_χ that decays with a rate Γ to a final state with a photon of energy $E_\gamma = h\nu_0$. We assume here the particle to be long-lived compared with the age of the Universe (i.e., $\Gamma \lesssim H_0 \simeq 10^{-18}\,\mathrm{sec}^{-1}$) so that the density of the decaying particles is $\rho_\chi(t) = \rho_{\chi 0} a^{-3}$ with the scale factor $a(t)$ (normalized to $a(t_0) = 1$), given as a function of time t. Here $\rho_{\chi 0} = \rho_\chi(t_0)$, and t_0 is the time today. It is also conceivable that the Big Bang produced some other relic particle that decays with a lifetime $\tau = \Gamma^{-1} \lesssim H_0^{-1}$ and IM can be used to seek such short-lived particles as well, although we do not consider this possibility here.

A. Isotropic specific intensity

We now calculate the isotropic specific intensity of decay photons today. The specific luminosity density (energy density per unit time per unit frequency interval) due to decays is $\epsilon_\nu(t) = \zeta\Gamma\rho_\chi(t)\theta(\nu-\nu_0)$, where $\zeta = (h\nu_0/m_\chi c^2)$ is the fraction of energy transferred away to photons, and $\theta(\nu)$ is the line profile of the signal.[1] We take $\theta(\nu)$ to be the Dirac delta function. The specific intensity observed at frequency ν and $z = 0$ is given by the solution [31, 32],

$$I_\nu = \frac{1}{4\pi}\int_0^\infty dz \frac{c}{H(z)} \frac{\epsilon_{\nu(1+z)}(z)}{(1+z)^4}, \tag{1}$$

to the radiative-transfer equation, where $H(z)$ is the Hubble parameter at redshift z, and we have used z as a proxy for t. For dark-matter-decay photons, this expression evaluates to

$$I_\nu = \frac{c}{4\pi\nu_0}\frac{\Gamma}{H_0}\frac{\rho_\chi(z)}{E(z)(1+z)^4}\bigg|_{z=\frac{\nu_0}{\nu}-1}, \tag{2}$$

where $H(z) \equiv H_0 E(z)$, and for ΛCDM, $E(z) = \left[\Omega_m(1+z)^3 + (1-\Omega_m)\right]^{1/2}$, with Ω_m the matter-density parameter today. Using $\rho_{\chi 0} = f\Omega_c\rho_c$, where ρ_c is the critical energy density of the Universe, Ω_c the fraction of critical density in dark matter, and f the fraction of dark matter today in decaying particles, the specific intensity evaluates, using Planck 2015 parameters, to

$$\nu I_\nu = 2.4\times 10^{-3}\,\mathrm{W\,m^{-2}\,sr^{-1}}\;\frac{\nu}{\nu_0}\frac{\Gamma}{H_0}\frac{f\zeta}{E(z)\,(1+z)}\bigg|_{z=\frac{\nu_0}{\nu}-1}. \tag{3}$$

The intensity is nonzero only for frequencies $\nu \le \nu_0$.

The specific fluence (number flux of photons, over all directions, per unit frequency interval) is $F_\nu = 4\pi I_\nu/(h\nu)$, and the total fluence (over all photon directions) is $F = \int F_\nu\, d\nu$. For example, for $f = 1$, $m_\chi c^2 = 1$ eV, $\zeta = 1/2$, and $\Gamma = H_0$, the total fluence evaluates to $2.9\times 10^{17}\ \mathrm{m^{-2}\ sec^{-1}}$.

B. Cross-correlation with mass distribution

Photons from dark-matter decay must be distinguished from a huge background of photons in the extragalactic background. We propose here to use the cross-correlation of these decay photons (which trace the dark-matter distribution) with some tracer of the large-scale mass distribution to distinguish decay photons from those in the extragalactic background.

We now calculate the smallest number of decay photons that need to be detected to establish their correlation with large-scale structure. To do so, we assume that we have sampled the distribution of mass over a cosmological volume V with a matter-tracer population (e.g., galaxies) that has a mean number density $\bar{n}_g$ and bias b. The fractional mass-density perturbation is $\delta(\vec{x})$ with Fourier transform $\tilde{\delta}(\vec{k}) = \int d^3x\, \delta(\vec{x})e^{i\vec{k}\cdot\vec{x}}$, so that the matter power spectrum $P(k)$ is then obtained from $\left\langle \tilde{\delta}(\vec{k})\delta^*(\vec{k}')\right\rangle = (2\pi)^3\delta_D(\vec{k}-\vec{k}')P(k)$, with $\delta_D(\vec{k})$ the 3-dimensional Dirac delta function. The power spectrum for the tracer population is $b^2P(k) + \bar{n}_g^{-1}$, where we have added a Poisson contribution due to the finite number density of the tracer population [32].

The same matter-density field is also sampled in the IM experiment by the photons observed from dark-matter decay. We surmise that there are $N_\chi = \xi N_\gamma$ such photons that appear in the experiment, in addition to $N_b = (1-\xi)N_\gamma$ photons from the extragalactic background light (EBL), the integrated light from galaxies. Here N_γ is the total number of observed photons, and the EBL has a frequency spectrum described in Refs. [24, 33, 34]. The galaxies that give rise to this EBL are a biased tracer of the mass distribution and so will also be clustered. However, the light from a given galaxy is broadly distributed over frequencies and so the EBL-photon distribution in the IM angular-frequency space is smoothed. We therefore suppose that the background photons are uniformly distributed throughout the volume. We also add to the EBL, for measurements at frequencies $\nu \lesssim 100$ GHz, Galactic synchrotron radiation, which we model roughly in terms of a brightness temperature $T_B = 1000\,\mathrm{K}\,(\nu/100\,\mathrm{MHz})^{-2.5}$.

The fractional luminosity density perturbation in the *observed* photon population is then $\delta_\gamma = N_\chi/(N_\chi + N_b)\delta = \xi\tilde{\delta}$. It follows that the cross-correlation between the observed photons and tracers is

$$\left\langle \tilde{\delta}_g(\vec{k})\tilde{\delta}^*_\gamma(\vec{k}')\right\rangle = (2\pi)^3\delta_D(\vec{k}-\vec{k}')\,\xi b P(k); \tag{4}$$

i.e., the photon-tracer cross-correlation has a power spectrum $P_{g\gamma}(k) = b\xi P(k)$.

[1] If the particle, like the axion, decays to two photons, this expression is multiplied by 2. Thus, two-photon decays can be accommodated in all subsequent expressions by replacing $\zeta \to 2\zeta$.

To seek this cross-correlation, we take the Fourier amplitudes $\tilde{\delta}_g(\vec{k})$ (from the tracer survey) and $\tilde{\delta}_\gamma(\vec{k})$ (from the IM experiment, for some nominal decay frequency ν_0) for each wavevector $\vec{k}$. Their product then provides an estimator for $P_{g\gamma}(k)$ with variance,

$$\left[P_{g\gamma}(k)\right]^2 + \left[P_{\gamma\gamma}(k) + \bar{n}_\gamma^{-1}\right]\left[P_{gg}(k) + \bar{n}_g^{-1}\right]. \tag{5}$$

Here, $\bar{n}_\gamma = N_\gamma/V$ is the number of photons collected divided by the volume surveyed, and $P_{\gamma\gamma}(k) = \xi^2 P(k)$. If we write $P(k) = Ak^{n_s}\left[T(k)\right]^2$, in terms of the scalar spectral index $n_s \simeq 0.96$, the ΛCDM transfer function $T(k)$, and amplitude A, then the estimator from this Fourier mode for $P_{g\gamma}(k)$ provides an estimator for the product ξb, and thus (if b is known) for ξ. The minimum-variance estimator for ξ is then obtained by adding the estimators from each $\vec{k}$ mode with inverse-variance weighting.

Since the signal for each Fourier mode is $\xi b P(k)$, the squared signal-to-noise with which the cross-correlation can be measured with the minimum-variance estimator is

$$\left(\frac{S}{N}\right)^2 = \sum_{\vec{k}} \frac{\left[\xi b P(k)\right]^2/2}{\left[\xi b P(k)\right]^2 + \left(\xi^2 P(k) + \bar{n}_\gamma^{-1}\right)\left(b^2 P(k) + \bar{n}_g^{-1}\right)}. \tag{6}$$

To distinguish a detection from the null hypothesis $\xi = 0$, we evaluate the noise under this null hypothesis and then estimate the sum by approximating $b^2P(k)/\left[b^2P(k)+\bar{n}_g^{-1}\right] = 1$ for $b^2P(k) > \bar{n}_g^{-1}$ and $b^2P(k)/\left[b^2P(k)+\bar{n}_g^{-1}\right] = 0$ for $b^2P(k) < \bar{n}_g^{-1}$. Doing so, we find that the cross-correlation between decay photons and the tracer population can be measured with a signal to noise

$$(S/N) = \xi\sqrt{N_b\sigma_k^2/2}, \tag{7}$$

where $\sigma_k^2 \simeq (2\pi^2)^{-1}\int^{k_{\rm max}} k^2 P(k)\, dk$ is the variance of the mass distribution on a distance scale $k_{\rm max}^{-1}$ determined from $P(k_{\rm max}) = (b^2\bar{n}_g)^{-1}$. Fig. 1 shows the dependence of σ_k on the tracer number density $\bar{n}_g$ and its bias b.

Since the scheme suggested here involves *cross*-correlation of a putative decay line with a tracer of the matter distribution, the measurement is limited *not* by the number of Fourier modes of the density field that can be well sampled, but only by the fidelity with which the density field can be sampled and by the number of photons observed. Moreover, the factor σ_k^2 in any measurement is really the variance of the density field, as determined by the tracer survey, in the volume surveyed.

The condition for a $\gtrsim 2\sigma$ detection of a decay-line signal is

$$\xi \gtrsim \xi_{\rm min} \simeq 2(N_b\sigma_k^2/2)^{-1/2}. \tag{8}$$

Since the intensity I_ν from dark-matter decay and the EBL intensity $I_\nu^{\rm CB}$ both vary smoothly with frequency, we approximate $\xi = N_\chi/(N_\chi + N_b) \simeq N_\chi/N_b$ as $\xi \simeq I_\nu/I_\nu^{\rm CB}$. We then require, for detection of a signal, $I_{\nu_0} \gtrsim \xi_{\rm min} I_{\nu_0}^{\rm CB}$, with I_ν taken from Eq. (3), and evaluated at the frequency ν_0 at which (for $\Gamma \lesssim H_0$) it peaks. A cross-correlation can then be detected if the decay lifetime is

$$\begin{aligned}\tau \equiv \Gamma^{-1} &\lesssim \frac{f\zeta H_0^{-1}c}{8\sqrt{2}\pi}\sqrt{N_b\sigma_k^2}\left[\frac{\Omega_c\rho_c}{\nu_0 I_{\nu_0}^{\rm CB}}\right] \\ &\simeq 7.5\times 10^{32}\frac{f\zeta\sigma_k(N_b/10^{20})^{1/2}}{(\nu_0 I_{\nu_0}^{\rm CB}/10^{-8}\ {\rm W\ m^{-2}\ sr^{-1}})}\ {\rm sec.}\end{aligned} \tag{9}$$

Here, N_b is the number of EBL photons from the fraction $f_{\rm sky}$ of the sky observed with frequencies $\nu_1 \leq \nu \leq \nu_2$ that cross a detector area A in time T; i.e.,

$$N_b = 4\pi f_{\rm sky} A T\int_{\nu_1}^{\nu_2} d\nu\, I_\nu^{\rm CB}/(h\nu). \tag{10}$$

C. Order-of-magnitude estimates and scalings

We now work out some order-of-magnitude estimates. Consider a tracer survey that samples galaxies in a volume to redshift $z \sim 1$, over $f_{\rm sky}$ of the sky. If the galaxy density is $\gtrsim 0.01$ Mpc^{-3}, then we will have, $k_{\rm max} \gtrsim 0.1$ Mpc^{-1}, for which $\sigma_k \gtrsim 1$ (and we take $b \sim 1$). We consider an intensity-mapping experiment with a frequency range broad enough to detect decay photons over the redshift range $0 \leq z \leq 1$, and at frequencies $\nu \sim 10^{14}$ Hz (roughly optical, probed by SPHEREx). From Fig. 9 in Ref. [34] we ballpark (conservatively) the EBL intensity as $\nu I_\nu^{\rm CB} \sim 10^{-8}$ W m^{-2} sr^{-1} and fluence (over all photon directions) as 10^{12} m^{-2} s^{-1}. We imagine a detector of area $A_{\rm m}$ m^2 and observation time $T_{\rm yr}$ yr. From Eq. (7), we then estimate the smallest detectable fraction of decay photons ξ to be $\xi_{\rm min} \sim 5\times10^{-10}(f_{\rm sky}A_{\rm m}T_{\rm yr})^{-1/2}$ (at 2σ). Comparing the EBL fluence with our prior result, $\sim 3\times10^{17}$ m^{-2} s^{-1}, for the fluence from dark-matter decay with $h\nu_0 \sim$ eV, $f\zeta = 1/2$, and $\Gamma = H_0$, we infer the largest detectable lifetime for such a measurement to be

$$\tau_{\rm max} \simeq 10^{33}\, f\zeta(f_{\rm sky}A_{\rm m}T_{\rm yr})^{1/2}{\rm sec.} \tag{11}$$

Note that this is $\xi_{\rm min}^{-1} \sim 10^9$ times better than the limit inferred by simply requiring the decay-line intensity to be smaller than the observed EBL intensity at ν_0 and $\sim 10^8$ times better than the strongest current bounds from null searches for decay lines from galaxy clusters [29].

As Eq. (11) indicates the sensitivity scales with the square root of the area on the sky, the area of the detector, and the duration of the experiment—i.e., with the square root of the the total number of background photons—as expected. There is also a dependence on σ_k, although this is weak. As Fig. 1 shows, the dependence of σ_k with $k_{\rm max}$ is roughly linear for values $k_{\rm max} \sim 0.1$ Mpc^{-1}, and $\tau_{\rm max}$ depends linearly on σ_k: a greater density contrast makes a cross-correlation more easily detectable.

The linear-theory calculation here may be seen as conservative, given that nonlinear evolution enhances the power spectrum on smaller scales. On the other hand, as one goes to smaller scales, the fidelity with which a population traces the mass distribution decreases. The numerical estimate above, which used a value $\sigma_k \sim 1$, makes the conservative assumption that only information from the linear regime is used.

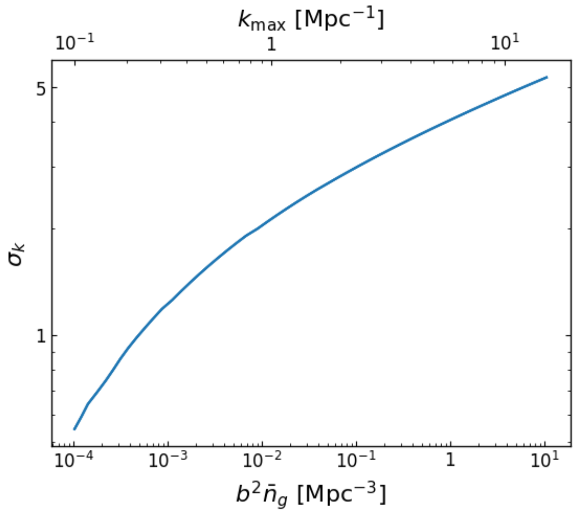

FIG. 1. The dependence of the mass-density root-variance σ_k on the tracer-population spatial density $\bar{n}_g$ and its bias b.

III. FORECASTS FOR EXPERIMENTS

To make the next step in connection to realistic experiments, we now consider the spatial resolution of the experiment and, moreover, the anisotropy in the spatial resolution of the cosmic volume probed. This anisotropy arises because the spatial resolution of the experiment in the radial direction is fixed by the frequency resolution; this most generally differs from the spatial resolution in directions transverse to the line of sight, which are fixed by the angular resolution. To account for these effects, we define wavenumbers $k_{\rm max,||}$ and $k_{\rm max,\perp}$ in the line-of-sight and transverse directions, respectively. These are fixed by the frequency and angular resolutions of the experiment. If these wavenumbers are larger than $k_{\rm max}$ from the finite tracer number density (discussed above), then the effective resolution is fixed by finite tracer number density. If they are smaller, then the resolution is fixed by the survey resolutions. That is, we replace the $k_{\rm max}$ we derived above by

$$\begin{aligned}\tilde{k}_{\rm max,||} &\equiv \min\left[k_{\rm max}, k_{\rm max,||}\sqrt{1-(k_\perp/k_{\rm max,\perp})^2}\right],\\ \tilde{k}_{\rm max,\perp} &\equiv \min\left[k_{\rm max}, k_{\rm max,\perp}\right],\end{aligned} \tag{12}$$

and then model the Fourier-space volume as an ellipse with the corresponding principal semi-axes. Explicitly, this is

$$\sigma_k^2 = \frac{1}{2\pi^2}\int^{\tilde{k}_{\rm max,\perp}}\int^{\tilde{k}_{\rm max,||}} k_\perp P\left(\sqrt{k_{||}^2+k_\perp^2}\right) dk_\perp dk_{||}. \tag{13}$$

The maximum parallel and perpendicular wavenumbers are most generally redshift-dependent, and if so, then we need an integration in Eq. (7) also over cocentric ellipsoidal shells with thickness given by the spectral resolution and parametrized by redshift. However, given the rough nature of our calculation, we approximate the wavenumbers as constant in redshift as

$$\begin{aligned}k_{\rm max,||} &= RH(z)/[c(1+z)] \approx RH_0/c,\\ k_{\rm max,\perp} &= [r_c(z)\theta_{\rm res}]^{-1} \approx [r_c(0)\theta_{\rm res}]^{-1},\end{aligned} \tag{14}$$

where $r_c(z)$ is the comoving size of the Universe at redshift z, R the spectral resolution, and $\theta_{\rm res}$ the pixel resolution of the experiment.

The last step is to estimate the effects of instrumental noise on the measurement. We do so by supposing that instrument noise distributes $N_{\rm n}$ photons, in addition to the N_b EBL photons, uniformly in the survey volume. The fraction ξ of decay photons from the sky now gets replaced by a fraction $\xi^{\rm obs} = N_\chi/(N_\chi + N_b + N_{\rm n}) = \xi(N_\chi + N_b)/(N_\chi + N_b + N_{\rm n})$ of the observed (decay plus EBL plus instrumental-noise) photons that come from decays. Following the same reasoning as above, the smallest detectable $\xi^{\rm obs}$ is $\xi^{\rm obs}_{\rm min} = 2\sqrt{2}\sqrt{N_b+N_{\rm n}}/(N_b\sigma_k)$. The expression, Eq. (8), for the smallest detectable ξ, then becomes,

$$\xi_{\rm min} \simeq 2(N_b\sigma_k^2/2)^{-1/2}\sqrt{1+(N_{\rm n}/N_b)}, \tag{15}$$

after taking into account the $N_{\rm n}$ additional noise photons. We can estimate the ratio $(N_{\rm n}/N_b) \simeq (I_\nu^{\rm n}/I_\nu^{\rm CB})$ in terms of an instrument-noise intensity $I_\nu^{\rm n}$ which can be parameterized in terms of the Planck function $B_\nu(T_{\rm eff})$ at a given effective system temperature $T_{\rm eff}$. As Eq. (15) indicates, if $I_{\nu_0}^{\rm n} \lesssim I_{\nu_0}^{\rm CB}$, then instrument noise does not degrade the sensitivity. if $I_{\nu_0}^{\rm n} \gtrsim I_{\nu_0}^{\rm CB}$, then instrument noise reduces the smallest detectable τ, given in Eq. (9), by a factor $(I_{\nu_0}^{\rm CB}/I_{\nu_0}^{\rm n})^{1/2}$.

We now use Eq. (9), the cosmic background photon distribution in Ref. [34], and the experimental parameters shown in Table I to forecast lifetime sensitivities for an array of intensity-mapping experiments that are being pursued or under consideration. The array of experiments is chosen to illustrate the different frequencies (and the principle target astrophysical emission lines) being targeted by current intensity-mapping efforts. The representative efforts are CHIME [35], CCAT-prime [36]; COMAP [37]; STARFIRE [38]; and SPHEREx [39]. There are, however, a number of other projects, and several other lines, in other frequency windows, that may be targets for IM efforts—see Ref. [27] for a more comprehensive list. We also caution that the planning for some experiments is not yet complete, and so the detailed parameters may change.

The results are shown in Fig. 2. The experimental parameters we use for these estimates are the survey exposure, the frequency ranges probed, the sky coverage, and the angular/frequency resolutions. We include the dependence of the redshift range probed via the emitted photon's energy and observed frequency range. We assume that that $\sigma_k = 2.3$ for some tracer population (corresponding to $k_{\max} = 1.2$ Mpc^{-1}), but take into account the (possibly direction-dependent) modification of $k_{\max}$ determined by the angular and frequency resolution of the experiment. For each experiment, we show two curves, one that includes the estimated effects of instrumental noise, and another, more optimistic, curve that indicates the limit, from the EBL, for an experiment with similar exposure and sky and frequency coverage, but with no instrumental noise. We also plot in Fig. 2 a current conservative lower bound to τ inferred simply by demanding that the decay-line intensity be less than the observed EBL intensity at ν_0.

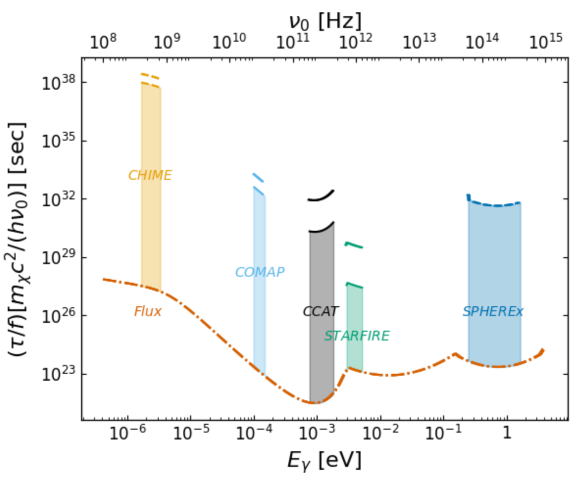

FIG. 2. The largest lifetime τ for which a decay signal can be detected for the experiments shown. Here, f is the fraction of the dark matter composed of the particle that undergoes decays, m_χ the mass of the decaying particle, E_γ the decay-photon (rest-frame) energy, and ν_0 the decay-photon rest-frame frequency. The line labeled "Flux" is the largest lifetime consistent with the requirement that the intensity from particle decays does not exceed the extragalactic background light (EBL) intensity. The shaded regions are those not yet ruled out by current EBL measurements that will be accessible, given our estimates of the instrumental noise, with each experiment. The curves above each experiment (except for SPHEREx, which is limited by the EBL, not instrument noise) show the best sensitivity achievable with an experiment with similar specifications, but no instrumental noise, the sensitivity being limited in this case by the EBL. The experimental parameters assumed for each experiment are listed in Table I.

IV. DISCUSSION

As Fig. 2 indicates, IM experiments have the potential to dramatically increase our ability to seek radiatively-decaying dark matter in several photon energy windows, even with current-generation experiments. Our discussion above supposed that the cosmic mass distribution, against which the decay-line signal is to be cross-correlated, is obtained from a tracer survey of number density $\bar{n}_g$. However, the mass distribution is likely to be obtained, over the relevant cosmic volumes, by the intensity-mapping experiment itself. If so, then the relevant value of σ_k is that at which the contribution $P_{\rm n}(k)$ of the measurement noise (which may come from shot noise in the emitting sources and/or instrumental noise) to the power spectrum overtakes the tracer power spectrum $b^2P(k)$; i.e., $P_{\rm n}(k_{\max}) = b^2P(k_{\max})$. If the decay-line signal is sought by cross-correlation with a given galactic/IGM emission line, then our proposed search algorithm resembles that, proposed in Ref. [40], to seek a faint ^{13}CO line through cross-correlation with the brighter ^{12}CO line.

We neglected residual correlations in the EBL photons due to clustering of their sources, since the smoothing of the galaxy distribution along the line of sight, due to the broad galaxy spectrum, will suppress these. We believe that these residual correlations will be most generally be small, since the dynamic range of the frequency coverage for most IM mapping experiments is not too much greater than the width of the galaxy frequency spectrum. There may also be spectrum-mapping techniques, where emission from different frequencies of a characteristic galaxy spectrum are correlated, that can be used to mitigate the contamination from EBL clustering. The precise sensitivity is likely to be frequency dependent and weakened considerably if the decay-line frequencies coincides with that of a strong galactic emission line.

Let us now apply our results to the case of an axion that decays to two photons. To do so, we set $\zeta = 1/2$ and replace $\zeta \to 2\zeta$ due to there being two decay photons. For axions, there is a constraint $\tau \gtrsim 1.9 \times 10^{26}\,(m_a c^2/\mathrm{eV})^{-3}$ sec, from horizontal-branch stars, over the mass ranges considered here. While this is stronger than the sensitivities forecast here for $2E_\gamma = m_a c^2 \lesssim 0.1$ eV, it is considerably weaker than the sensitivity with SPHEREx we anticipate for $m_a c^2 \sim$ eV. The horizontal-branch constraint will not, however, necessarily apply more generally to other particles that undergo radiative decay. Scenarios where a heavier particle decays to a lighter state (e.g., as in exciting dark matter [21]) have appeared, motivated by a variety of problems, with a variety of dark-matter masses, decay-photon energies, and detailed implementations; see, e.g., Refs. [41–47]. For example, suppose, following these references, that the dominant dark-matter component is a doublet (χ_1, χ_2) of mass m_χ that consists of two different mass states with a mass splitting $\Delta m \ll m_\chi$ which is then equal to the energy of the resulting decay photon. If, for

Experiment	target	$[\nu_1, \nu_2]$ (GHz)	A (m^2)	$f_{\rm sky}$	R	$\theta_{\rm res}$	$T_{\rm eff}$ K
CCAT	[CII] (high z)	$[185, 440]$	28	3.9×10^{-4}	300	$1'$	148
CHIME	21-cm	$[400, 800] \times 10^{-3}$	8000	0.75	$\nu/(0.39$ MHz)	$20'$	100
COMAP	CO	$[26, 34]$	85	2.4×10^{-4}	800	$4'$	44
STARFIRE	[CII] (low z)	$[714, 1250]$	4.9	2.4×10^{-5}	250	1°	11
SPHEREx	Hα	$[60, 400] \times 10^3$	0.031	1	$41.4, 135^*$	$6.2''$	$0^\dagger$

TABLE I. The experiment parameters used in Fig. 2. The survey duration in each case was chosen to be one year. *SPHEREx has two spectral resolutions, one for the low-frequency channels and another at high frequencies. †The noise in SPHEREx is limited by zodiacal light and turns out, for our purposes, to be negligible compared with that contributed by the EBL.

example, we surmised $m_\chi c^2 \sim$ GeV and required that $\tau \gtrsim 10^{18}$ sec, then Fig. 2 indicates that the signal from $\sim 10^{-5}$ eV decay photons could be detected by CHIME even if the decay lifetime were as large as $\tau \sim 10^{24}$ sec. We leave the identification, exploration, and development of such models to future work.

We have assumed in our analysis that the particles undergo vacuum decay with a rate Γ. The entire discussion applies *mutatis mutandis*, however, for annihilations. In this case, Γ may have some slow redshift evolution which must be taken into account, and the annihilation-rate density fluctuation may be biased relative to the fluctuation in the dark-matter density. We leave further elaboration of these details, as well as investigation of detailed particle-physics models with such a signature to future work.

To close, we have suggested that lines from dark-matter decay and annihilation can be sought by cross-correlating a line signature in intensity-mapping experiments with some tracer of the mass distribution. We have sketched how such a cross-correlation can be performed and presented simple forecasts for the sensitivities that can, in principle, be achieved. Since intensity mapping is only now getting underway, with long-term experimental capabilities yet to be specified in detail, our estimates are for hypothetical experiments limited only by the unavoidable noise presented by extragalactic background light. The potentially extraordinary improvements to the sensitivity to lines from dark-matter decay or annihilation we have shown motivates more careful feasibility studies and adds to the already strong scientific motivation, from more traditional astrophysics and cosmology [27, 39], to pursue intensity mapping.

ACKNOWLEDGMENTS

We thank Patrick Breysse, Ely Kovetz, and an anonymous referee for useful comments on earlier drafts. CS acknowledges the support of the Bill and Melinda Gates Foundation, Anna Salzberg, and Albert Ratner. This work was supported by NASA Grant No. NNX17AK38G, NSF Grant No. 0244990, and the Simons Foundation.

[1] P. A. R. Ade *et al.* [Planck Collaboration], "Planck 2015 results. XIII. Cosmological parameters," Astron. Astrophys. **594**, A13 (2016) [arXiv:1502.01589 [astro-ph.CO]].

[2] G. Hinshaw *et al.* [WMAP Collaboration], "Nine-Year Wilkinson Microwave Anisotropy Probe (WMAP) Observations: Cosmological Parameter Results," Astrophys. J. Suppl. **208**, 19 (2013) [arXiv:1212.5226 [astro-ph.CO]].

[3] B. J. Carr and S. W. Hawking, "Black holes in the early Universe," Mon. Not. Roy. Astron. Soc. **168**, 399 (1974).

[4] S. Bird, I. Cholis, J. B. Muñoz, Y. Ali-Haïmoud, M. Kamionkowski, E. D. Kovetz, A. Raccanelli and A. G. Riess, "Did LIGO detect dark matter?," Phys. Rev. Lett. **116**, no. 20, 201301 (2016) [arXiv:1603.00464 [astro-ph.CO]].

[5] S. Clesse and J. García-Bellido, "The clustering of massive Primordial Black Holes as Dark Matter: measuring their mass distribution with Advanced LIGO," Phys. Dark Univ. **15**, 142 (2017) [arXiv:1603.05234 [astro-ph.CO]].

[6] M. S. Turner, "Windows on the Axion," Phys. Rept. **197**, 67 (1990).

[7] G. G. Raffelt, "Astrophysical methods to constrain axions and other novel particle phenomena," Phys. Rept. **198**, 1 (1990).

[8] D. Cadamuro and J. Redondo, "Cosmological bounds on pseudo Nambu-Goldstone bosons," JCAP **1202**, 032 (2012) [arXiv:1110.2895 [hep-ph]].

[9] G. Carosi, A. Friedland, M. Giannotti, M. J. Pivovaroff, J. Ruz and J. K. Vogel, "Probing the axion-photon coupling: phenomenological and experimental perspectives. A snowmass white paper," arXiv:1309.7035 [hep-ph].

[10] D. J. E. Marsh, "Axion Cosmology," Phys. Rept. **643**, 1 (2016) [arXiv:1510.07633 [astro-ph.CO]].

[11] A. Kusenko, "Sterile neutrinos: The Dark side of the light fermions," Phys. Rept. **481**, 1 (2009) [arXiv:0906.2968 [hep-ph]].

[12] G. Jungman, M. Kamionkowski and K. Griest, "Supersymmetric dark matter," Phys. Rept. **267**, 195 (1996) [hep-ph/9506380].

[13] L. Bergström, "Nonbaryonic dark matter: Observational evidence and detection methods," Rept. Prog. Phys. **63**, 793 (2000) [hep-ph/0002126].

[14] D. Hooper and S. Profumo, "Dark matter and collider phenomenology of universal extra dimensions," Phys.

Rept. **453**, 29 (2007) [hep-ph/0701197].

[15] K. M. Zurek, "Asymmetric Dark Matter: Theories, Signatures, and Constraints," Phys. Rept. **537**, 91 (2014) [arXiv:1308.0338 [hep-ph]].

[16] G. Bertone, D. Hooper and J. Silk, "Particle dark matter: Evidence, candidates and constraints," Phys. Rept. **405**, 279 (2005) [hep-ph/0404175].

[17] K. Kaneta, H. S. Lee and S. Yun, "Portal Connecting Dark Photons and Axions," Phys. Rev. Lett. **118**, no. 10, 101802 (2017) [arXiv:1611.01466 [hep-ph]].

[18] D. Ejlli, "Axion mediated photon to dark photon mixing," Eur. Phys. J. C **78**, no. 1, 63 (2018) [arXiv:1609.06623 [hep-ph]].

[19] K. Choi, S. Lee, H. Seong and S. Yun, "Gamma-ray spectral modulations induced by photon-ALP-dark photon oscillations," arXiv:1806.09508 [hep-ph].

[20] L. Marzola, M. Raidal and F. R. Urban, "Oscillating Spin-2 Dark Matter," Phys. Rev. D **97**, no. 2, 024010 (2018) [arXiv:1708.04253 [hep-ph]].

[21] D. P. Finkbeiner and N. Weiner, "Exciting Dark Matter and the INTEGRAL/SPI 511 keV signal," Phys. Rev. D **76**, 083519 (2007) [astro-ph/0702587].

[22] M. T. Ressell, "Limits to the radiative decay of the axion," Phys. Rev. D **44**, 3001 (1991).

[23] M. Kamionkowski, "Diffuse gamma-rays from WIMP decay and annihilation," astro-ph/9404079.

[24] J. M. Overduin and P. S. Wesson, "Dark matter and background light," Phys. Rept. **402**, 267 (2004) [astro-ph/0407207].

[25] S. Furlanetto, S. P. Oh and F. Briggs, "Cosmology at Low Frequencies: The 21 cm Transition and the High-Redshift Universe," Phys. Rept. **433**, 181 (2006) [astro-ph/0608032].

[26] M. F. Morales and J. S. B. Wyithe, "Reionization and Cosmology with 21 cm Fluctuations," Ann. Rev. Astron. Astrophys. **48**, 127 (2010) [arXiv:0910.3010 [astro-ph.CO]].

[27] E. D. Kovetz *et al.*, "Line-Intensity Mapping: 2017 Status Report," arXiv:1709.09066 [astro-ph.CO].

[28] M. A. Bershady, M. T. Ressell and M. S. Turner, "Telescope search for multi-eV axions," Phys. Rev. Lett. **66**, 1398 (1991).

[29] D. Grin, G. Covone, J. P. Kneib, M. Kamionkowski, A. Blain and E. Jullo, "A Telescope Search for Decaying Relic Axions," Phys. Rev. D **75**, 105018 (2007) [astro-ph/0611502].

[30] Y. Gong, A. Cooray, K. Mitchell-Wynne, X. Chen, M. Zemcov and J. Smidt, "Axion decay and anisotropy of near-IR extragalactic background light," Astrophys. J. **825**, no. 2, 104 (2016) [arXiv:1511.01577 [astro-ph.CO]].

[31] P. C. Breysse, E. D. Kovetz and M. Kamionkowski, "Carbon Monoxide Intensity Mapping at Moderate Redshifts," Mon. Not. Roy. Astron. Soc. **443**, no. 4, 3506 (2014) [arXiv:1405.0489 [astro-ph.CO]].

[32] A. R. Pullen, O. Doré and J. Bock, "Intensity Mapping across Cosmic Times with the $Ly\alpha$ Line," Astrophys. J. **786**, 111 (2014) [arXiv:1309.2295 [astro-ph.CO]].

[33] M. T. Ressell and M. S. Turner, "The Grand Unified Photon Spectrum: A Coherent View of the Diffuse Extragalactic Background Radiation," Comments Astrophys. **14**, 323 (1990) [Bull. Am. Astron. Soc. **22**, 753 (1990)].

[34] R. Hill, K. W. Masui and D. Scott, "The Spectrum of the Universe," The Universe **72**, 663 (2018) [arXiv:1802.03694 [astro-ph.CO]].

[35] K. Bandura *et al.*, "Canadian Hydrogen Intensity Mapping Experiment (CHIME) Pathfinder," Proc. SPIE Int. Soc. Opt. Eng. **9145**, 22 (2014) [arXiv:1406.2288 [astro-ph.IM]].

[36] www.ccatobservatory.org.

[37] T. Y. Li, R. H. Wechsler, K. Devaraj and S. E. Church, "Connecting CO Intensity Mapping to Molecular Gas and Star Formation in the Epoch of Galaxy Assembly," Astrophys. J. **817**, no. 2, 169 (2016) [arXiv:1503.08833 [astro-ph.CO]].

[38] A. Barlis, S. Hailey-Dunsheath, C. M. Bradford, C. McKenney, H. G. Le Duc, and J. Aguirre, "Development of low-noise kinetic inductance detectors for far-infrared astrophysics," APS April Meeting Abstracts, January 2017, abstract id. R4.007.

[39] O. Doré *et al.*, "Cosmology with the SPHEREX All-Sky Spectral Survey," arXiv:1412.4872 [astro-ph.CO].

[40] P. C. Breysse and M. Rahman, "Feeding cosmic star formation: Exploring high-redshift molecular gas with CO intensity mapping," Mon. Not. Roy. Astron. Soc. **468**, no. 1, 741 (2017) [arXiv:1606.07820 [astro-ph.GA]].

[41] F. Chen, J. M. Cline, A. Fradette, A. R. Frey and C. Rabideau, "Exciting dark matter in the galactic center," Phys. Rev. D **81**, 043523 (2010) [arXiv:0911.2222 [hep-ph]].

[42] H. An, M. Pospelov and J. Pradler, "Direct constraints on charged excitations of dark matter," Phys. Rev. Lett. **109**, 251302 (2012) [arXiv:1209.6358 [hep-ph]].

[43] D. P. Finkbeiner and N. Weiner, "X-ray line from exciting dark matter," Phys. Rev. D **94**, no. 8, 083002 (2016) [arXiv:1402.6671 [hep-ph]].

[44] H. Okada and T. Toma, "3.55 keV X-ray Line Signal from Excited Dark Matter in Radiative Neutrino Model," Phys. Lett. B **737**, 162 (2014) [arXiv:1404.4795 [hep-ph]].

[45] K. Schutz and T. R. Slatyer, "Self-Scattering for Dark Matter with an Excited State," JCAP **1501**, no. 01, 021 (2015) [arXiv:1409.2867 [hep-ph]].

[46] A. Berlin, A. DiFranzo and D. Hooper, "3.55 keV line from exciting dark matter without a hidden sector," Phys. Rev. D **91**, no. 7, 075018 (2015) [arXiv:1501.03496 [hep-ph]].

[47] A. Hektor, G. Hütsi, L. Marzola and V. Vaskonen, "Constraints on ALPs and excited dark matter from the EDGES 21-cm absorption signal," arXiv:1805.09319 [hep-ph].